Molecular Model for Solid-State Polymerization of Nylon 6. II. An Improved Model

MUKUND R. KULKARNI and SANTOSH K. GUPTA*

Department of Chemical Engineering, Indian Institute of Technology, Kanpur 208 016, India

SYNOPSIS

An improved mathematical model using the Vrentas–Duda theory for diffusion coefficients is developed for solid-state polymerization (SSP). This model is applied to nylon 6, and best-fit values of the parameters are obtained for this system using the Box complex analysis on available experimental data. The sensitivity of results to variations of these parameters is studied. It is found that the ring opening reaction can easily be omitted and the number of parameters thereby decreased. Detailed quantitative results are obtained to study the effects of changing the important operating conditions on SSP, e.g., intermediate remelting of nylon 6 powder, value of the water concentration (or level of vacuum) in the vapor phase, leaching of monomer and water before SSP, size and degree of crystallinity of polymer particles, etc. The diffusional effects on the rate constants are found to depend on a complex interplay of several important factors such as the generation of monomer and water by reaction, removal of water by macro-level diffusion, changes in the intrinsic rate constants due to decrease in the concentration of polymer molecules, etc. © 1994 John Wiley & Sons, Inc.

INTRODUCTION

It is often difficult to obtain extremely high molecular weight polymers by conventional melt polycondensations because of high melt viscosities and limitations posed by equilibrium. However, it is possible to raise the degree of polymerization (DP) of several step growth polymers by heating them in vacuum or in an inert gas at temperatures below their melting points but above their glass transition temperatures. This method, known as solid-state polymerization (SSP) is quite commonly used in industry. Applications involving stringent operating conditions (e.g., tire cords) and certain processing techniques such as blow molding and extrusion require such polymers. Both batch as well as continuous operations are being practiced in industry for this purpose, involving the use of fixed bed, rotary drum, and fluidized bed reactors.

Studies on SSP go back to the early 1940s. Most of the early information is in the form of patents. Work on SSP started getting reported in the open literature about two decades ago.[1-4] Gaymans et al.[5] carried out a systematic experimental study on the SSP of nylon 6, while Griskey and Lee[4] and Chen et al.[1] provided some experimental data on nylon 66 and on nylon 6–10 and polyethylene terephthalate, respectively, under a variety of conditions. Pilati[6] and Fakirov[7] have provided excellent reviews of the work in this area.

Most of the early studies provided semiempirical models to explain experimental data. Kumar et al.[8] proposed a phenomenological model having a molecular basis to explain some important trends observed in the SSP of condensation polymers. They adapted the model of Chiu et al.[9] for the gel effect in free radical polymerizations, to SSP. More recently, Kaushik and Gupta[10] extended and improved this model and applied it to the SSP of nylon 6. They obtained curve-fitted values of the parameters in their model, using the experimental data of Gaymans et al.[5] In the present study, we present a new model, which uses the free volume theory of Vrentas and Duda[11] to account for the changes in the diffusion coefficients more accurately, using parameters that can be obtained directly from independent ex-

* To whom correspondence should be addressed.

Journal of Applied Polymer Science, Vol. 53, 85–103 (1994)
 CCC 0021-8995/94/010085-19

periments that do not involve reactions. This model, applicable to any reversible step growth polymerization in the presence of diffusional limitations, is applied to the specific case of the SSP of nylon 6 in this study. An optimal parameter estimation package is again used to obtain the best-fit values of the parameters used in this model, using the experimental data of Gaymans et al.[5]

FORMULATION

There are three major reversible reactions in the kinetic scheme of nylon 6 polymerization[12]: ring opening, polycondensation, and polyaddition. These are shown in Table I. The reaction most susceptible to diffusional limitations is the forward step of the polycondensation reaction, since it involves the diffusion of two large molecules toward each other. In SSP, however, it is expected that the diffusion of smaller molecules such as water and ε-caprolactam can also be affected. The present model takes this also into consideration. Thus, the reactions that are considered to be diffusion controlled in the present study are the forward and reverse steps of polycondensation, as well as the forward step of the polyaddition reaction, since at least one large molecule is involved in these three reactions. The backward steps of ring opening and polyaddition reactions are not diffusion controlled, since they involve only a single species. Similarly, the forward step of the ring opening reaction is assumed not to be diffusion controlled since it involves the diffusion of two small molecules.

We now model the variation of the forward rate constant of the polycondensation reaction associated with diffusional limitations. The approach used is similar to that suggested by Achilias and Kiparissides.[13,14] Figure 1 shows a polymer chain, P_m, with its functional A group at the center of a hypothetical sphere of radius $r_{m,1}$. Within this sphere, the effective concentration of polymer molecules is $[P]_m$. At a large distance, r_D, from the central functional group, the concentration of polymer molecules approaches the (local) bulk value, $[P]_b$. The reaction between the central functional A group and a B group of another polymer molecule, P_n, far away, occurs only after the latter comes in the vicinity of A by diffusion. The diffusion rate can be easily shown[9] to be independent of the radial location, and is given by

$$4\pi r^2 D_p \frac{d[P]}{dr} = C_1 \tag{1}$$

where D_p is the micro-level diffusivity of the polymer molecule in the medium. The following boundary conditions apply:

$$\text{at} \quad r = r_{m,1} \qquad [P] = [P]_m \tag{2a}$$

$$\text{at} \quad r = r_D \to \infty \qquad [P] = [P]_b \tag{2b}$$

Equations (1) and (2) give

$$4\pi D_p r_{m,1}([P]_b - [P]_m) = C_1 \tag{3}$$

The rate of consumption of functional group B within the sphere of radius $r_{m,1}$, because of reaction between two large molecules (forward reaction of polycondensation step), is

$$\tfrac{4}{3}\pi r_{m,1}^3 (k_{2,0}[P]_m[P]_b) = C_1 \tag{4}$$

Table I Kinetic Scheme for Polymerization of Nylon 6

Ring opening

$$C_1 + W \underset{k_1'}{\overset{k_1}{\rightleftarrows}} P_1$$

Polycondensation

$$P_n + P_m \underset{k_2'}{\overset{k_2}{\rightleftarrows}} P_{n+m} + W$$

Polyaddition

$$P_n + C_1 \underset{k_3'}{\overset{k_3}{\rightleftarrows}} P_{n+1}$$

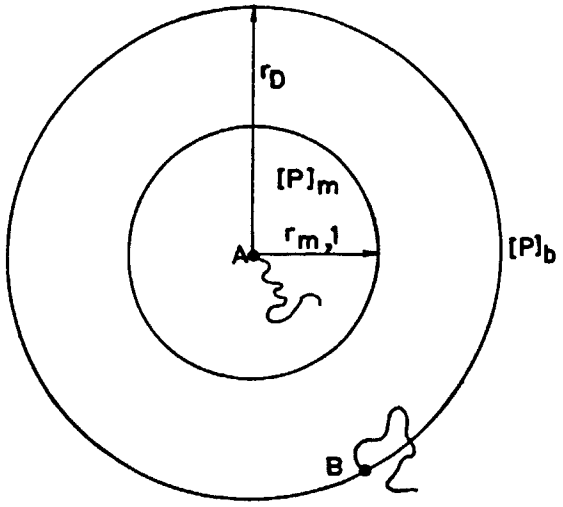

Figure 1 Segmental diffusion of a polymer molecule, P_n, with an unreacted B group toward another polymer molecule, P_m, with an unreacted A group.

Table II Apparent Reaction Rate Constants[a]

$$\frac{1}{k_2} = \frac{1}{k_{2,0}} + \theta_1(T)\mu_n^2\lambda_0 \frac{1}{\exp[-\chi + \chi_{ref}]}$$

$$\frac{1}{k_2'} = \frac{1}{k_{2,0}'} + \theta_2(T)\lambda_0 \frac{1}{\exp[\xi_{23}(-\chi + \chi_{ref})]}$$

$$\frac{1}{k_3} = \frac{1}{k_{3,0}'} + \theta_3(T)\lambda_0 \frac{1}{\exp[\xi_{13}(-\chi + \chi_{ref})]}$$

$$k_1 = k_{1,0} \quad k_1' = k_{1,0}' = k_{1,0}/K_1$$

$$k_3' = k_{3,0}' = k_{3,0}/K_3 \quad k_{2,0}' = k_{2,0}/K_2$$

$$\chi = \frac{\gamma\left\{\frac{\rho_m\phi_m\hat{V}_m^*}{\xi_{13}} + \frac{\rho_s\phi_s\hat{V}_s^*}{\xi_{23}} + \rho_p\phi_p\hat{V}_p^*\right\}}{\rho_m\phi_m\hat{V}_m^*V_{fm} + \rho_s\phi_s\hat{V}_s^*V_{fs} + \rho_p\phi_p\hat{V}_p^*V_{fp}}$$

$$\chi_{ref} = \frac{\gamma}{V_{fp}}$$

$$\xi_{13} = \frac{\hat{V}_m^*(\mathrm{MW}_m)}{\hat{V}_p^*M_{jp}}$$

$$\xi_{23} = \frac{\hat{V}_s^*(\mathrm{MW}_s)}{\hat{V}_p^*M_{jp}}$$

$$\rho_m = 1/\hat{V}_m^0(T) \quad \rho_p = 1/\hat{V}_p^0(T) \quad \rho_s = 1/\hat{V}_s^0(T)$$

$$\phi_m = \frac{[C_1](\mathrm{MW}_m)\hat{V}_m^0}{[C_1](\mathrm{MW}_m)\hat{V}_m^0 + \lambda_1(\mathrm{MW}_m)\hat{V}_p^0 + [W](\mathrm{MW}_s)\hat{V}_s^0}$$

$$\phi_p = \frac{\lambda_1(\mathrm{MW}_m)\hat{V}_p^0}{[C_1](\mathrm{MW}_m)\hat{V}_m^0 + \lambda_1(\mathrm{MW}_m)\hat{V}_p^0 + [W](\mathrm{MW}_s)\hat{V}_s^0}$$

$$\phi_s = \frac{[W](\mathrm{MW}_s)\hat{V}_s^0}{[C_1](\mathrm{MW}_m)\hat{V}_m^0 + \lambda_1(\mathrm{MW}_m)\hat{V}_p^0 + [W](\mathrm{MW}_s)\hat{V}_s^0}$$

[a] p, polymer; s, solvent (water); m, monomer (ϵ-caprolactam). Local bulk values of concentrations and moments used for all cases (subscript b not indicated).

where $k_{2,0}$ is the intrinsic rate constant for this reaction. Equations (3) and (4) give the expression for the effective polymer concentration at $r = r_{m,1}$ as

$$[P]_m = \frac{[P]_b}{1 + k_{2,0}\left\{\frac{r_{m,1}^2}{3D_p}\right\}[P]_b} \tag{5}$$

The overall rate of this reaction can also be written as $k_2[P]_b^2$, where k_2 is the apparent rate constant for this reaction, accounting for diffusional limitations as well. The two expressions for the rate give

$$k_2[P]_b^2 = k_{2,0}[P]_m[P]_b \tag{6}$$

On substituting the expression for $[P]_m$ from Eq. (5) in Eq. (6), we obtain

$$\frac{1}{k_2} = \frac{1}{k_{2,0}} + \left(\frac{r_{m,1}^2}{3D_p}\right)[P]_b \tag{7}$$

where $[P]_b$, the local bulk polymer concentration, can be rewritten in terms of the molecular weight distribution and its moments (see nomenclature) as

$$[P]_b = \sum_{n=1}^{\infty}[P_n]_b = \lambda_{0,b} \tag{8}$$

An analogous mathematical treatment for the backward step of the polycondensation reaction and the forward step of the polyaddition reaction leads to

$$\frac{1}{k_2'} = \frac{1}{k_{2,0}'} + \left(\frac{r_{m,2}^2}{3D_w}\right)[P]_b \tag{9a}$$

$$\frac{1}{k_3} = \frac{1}{k_{3,0}} + \left(\frac{r_{m,3}^2}{3D_m}\right)[P]_b \tag{9b}$$

where D_w and D_m are the effective micro-level diffusivities of water and monomer in the medium.

The free volume theory of Vrentas and Duda[11] can now be used for the diffusivities. The effective diffusivity, D_p, of polymer molecules can be written as

$$D_p = D_{p0}\mu_n^{-2}\exp\left(-\frac{E_p}{RT}\right)\exp(-\chi) \tag{10}$$

where

$$\chi = \frac{\gamma(\rho_m\phi_m\hat{V}_m^*/\xi_{13} + \rho_s\phi_s\hat{V}_s^*/\xi_{23} + \rho_p\phi_p\hat{V}_p^*)}{\rho_m\phi_m\hat{V}_m^*V_{fm} + \rho_s\phi_s\hat{V}_s^*V_{fs} + \rho_p\phi_p\hat{V}_p^*V_{fp}} \tag{11}$$

The same notation has been used here as in Ref. 13 (also see nomenclature). A semiempirical procedure is now used to simplify Eq. (10) further. A reference state is defined as $\phi_m \to 0$, $\phi_s \to 0$, and $\phi_p \to 1$. Equation (10) can be written in terms of the reference state (ref) as

$$\frac{1}{k_2} = \frac{1}{k_{2,0}} + \left(\frac{r_{m,1}^2}{3D_{p,ref}}\right)\lambda_0\frac{1}{D_p/D_{p,ref}}$$

$$= \frac{1}{k_{2,0}} + \left(\frac{r_{m,1}^2}{3D_{p,ref}\mu_{n,ref}^2}\right)\mu_n^2\lambda_0\exp(\chi - \chi_{ref})$$

$$\equiv \frac{1}{k_{2,0}} + \theta_1(T)\mu_n^2\lambda_0\exp(\chi - \chi_{ref}) \tag{12}$$

Table III Parameters Used to Calculate the Apparent Reaction Rate Constants

$(MW_m) = 0.11316$ kg/mol	
$(MW_s) = 0.018$ kg/mol	
$\hat{V}_m^* = 8.64 \times 10^{-4}$ m^3/kg	(Ref. 16)[a]
$\hat{V}_m^0$ (190°C) $= 11.325 \times 10^{-4}$ m^3/kg	(Ref. 16)[a]
$\hat{V}_p^* = 8.123 \times 10^{-4}$ m^3/kg	(Ref. 17)[a]
$\hat{V}_p^0(T) = \hat{V}_p^*[1 + V_{fp}(T)]$	
$\hat{V}_s^* = 9.69 \times 10^{-4}$ m^3/kg (water)	(Ref. 15)[a]
$\hat{V}_s^0$ (190°C) $= 11.429 \times 10^{-4}$ m^3/kg (water)	(Ref. 18)
V_{fm} (190°C) $= 0.31033$	(Ref. 16)[a]
V_{fs} (190°C) $= 0.1795$	(Refs. 15, 18)[a]
$V_{fp}(T) = 0.025 + (\alpha_l - \alpha_g)(T - T_g)$	(Refs. 19, 21)
$\frac{MW_m}{M_{jp}} = \frac{2}{3}$	(Ref. 20)
$\gamma = 1$	(Refs. 13, 14)
$\frac{1}{T_g} = \frac{1}{T_{g\infty}} + \frac{K_s}{T_{g\infty}^2}\frac{1}{\bar{\mu}_n}$	(Refs. 8, 19)
$T_{g\infty} = 350$ K	(Ref. 17)
$\alpha_l = 10^{-3}$ K^{-1}	(Refs. 17, 21)
$\alpha_g = 4.5 \times 10^{-4}$ K^{-1}	(Refs. 17, 21)
$K_s/T_{g\infty}^2 = 0.03$ K^{-1}	(Refs. 10)
$K_1 = \exp[(-32.989 - 8024.9/T)/\mathbb{R}]$	(Refs. 22)
$K_2 = \exp[(3.9846 + 2.4877 \times 10^4/T)/\mathbb{R}]$	(Refs. 22)
$K_3 = \exp[(-29.06 + 1.6919 \times 10^4/T)/\mathbb{R}]$	(Refs. 22)
$\mathbb{R} = 8.314$ J/mol K (gas constant)	

[a] Estimated values.

where

$$\chi_{ref} = \frac{\gamma}{V_{fp}} \tag{13}$$

The parameter, $\theta_1(T)$, is a function of temperature alone[13] for a given sample (it depends on the degree of crystallinity through the parameter $D_{p,ref}$). In a similar manner, Eq. (9) can be written as

$$\frac{1}{k_2'} = \frac{1}{k_{2,0}'} + \theta_2(T)\lambda_0 \exp[\xi_{23}(\chi - \chi_{ref})] \tag{14a}$$

$$\frac{1}{k_3} = \frac{1}{k_{3,0}} + \theta_3(T)\lambda_0 \exp[\xi_{13}(\chi - \chi_{ref})] \tag{14b}$$

Table II summarizes the final equations for the apparent rate constants. Numerical values of and correlations for the various parameters required have been compiled from various sources and are given in Table III along with references.[8,13-22] These parameters have been determined experimentally using independent measurements on nonreacting nylon 6 systems. The glass transition temperature of nylon 6 has been assumed to be a function of its spatially averaged value of the number-average chain length, $\bar{\mu}_n$, as assumed earlier.[8,10]

The micro-level diffusivity of water leads to a difference in the water concentrations at $r = r_{m,2}$ (where the concentration is $[W]_m$) and $r = r_D \rightarrow \infty$ (where the concentration is $[W]_b$). This gradient is accounted for in the expression for the apparent rate constant, k_2', in Eq. (14a). It may be pointed out that the bulk concentration of water, $[W]_b$, itself is not constant but varies with location due to the macro-level diffusion of water through the polymer pellet to the flowing inert gas outside. The diffusional resistance of W in the gas phase is neglected in this formulation. However, it is expected that there is considerable resistance for the diffusion of water within the pellet. We consider the reacting pellets to be spherical with the condensation by-product, W, diffusing radially outward. The macro-level diffusivity, $\mathbb{D}_w$, of W through the *solid* nylon 6 sphere is assumed to be constant. The mass balance equation for the spherical pellet with diffusion of W in the radial direction can be written as

Table IV Final Equations for Solid-State Polymerization of Nylon 6[a]

1. $\dfrac{\partial C_1}{\partial t} = -k_1 C_1 W + k_1' P_1 - k_3 C_1 \lambda_0 + k_3'(\lambda_0 - P_1)$

2. $\dfrac{\partial P_1}{\partial t} = k_1 C_1 W - k_1' P_1 - 2k_2 P_1 \lambda_0 + 2k_2' W(\lambda_0 - P_1) - k_3 P_1 C_1 + k_3' P_2$

3. $\dfrac{\partial \lambda_0}{\partial t} = k_1 C_1 W - k_1' P_1 - k_2 \lambda_0^2 + k_2' W(\lambda_1 - \lambda_0)$

4. $\dfrac{\partial \lambda_1}{\partial t} = k_1 C_1 W - k_1' P_1 + k_3 C_1 \lambda_0 - k_3'(\lambda_0 - P_1)$

5. $\dfrac{\partial \lambda_2}{\partial t} = k_1 C_1 W - k_1' P_1 + 2k_2 \lambda_1^2 + \frac{1}{3} k_2' W(\lambda_1 - \lambda_3) + k_3 C_1(\lambda_0 + 2\lambda_1) + k_3'(\lambda_0 - 2\lambda_1 + P_1)$

6. $\dfrac{\partial W}{\partial t} = -k_1 C_1 W + k_1' P_1 + k_2 \lambda_0^2 - k_2' W(\lambda_1 - \lambda_0) + D_w\left[\dfrac{\partial^2 W}{\partial r^2} + \dfrac{2}{r}\dfrac{\partial W}{\partial r}\right]$

Initial and Boundary Conditions

7. $t = 0$, values from Table V, independent of radial position

$r = 0 \qquad \dfrac{\partial W}{\partial r} = 0$

$r = R \qquad W = W_s$

Closure Conditions

8. $P_2 = P_1$
9. $\lambda_3 = \lambda_2(2\lambda_2\lambda_0 - \lambda_1^2)/(\lambda_1\lambda_0)$

[a] Brackets, [ ], for concentrations (local bulk values) omitted for brevity.

$$\frac{\partial [W]}{\partial t} = \mathbb{D}_w \frac{1}{r^2}\frac{\partial}{\partial r}\left(r^2 \frac{\partial [W]}{\partial r}\right) + \mathbb{R}_w \qquad (15)$$

where $\mathbb{R}_w$ is the rate of *generation* of water by chemical reaction (ring opening and polycondensation reactions) and is written as

$$\mathbb{R}_w = -k_1[C_1][W] + k_1'[P_1] + k_2\lambda_0^2 - k_2'(\lambda_1 - \lambda_0)[W] \qquad (16)$$

The complete set of mass balance and moment equations is given in Table IV. The initial conditions can be taken as a uniform distribution of W in the pellet, i.e., $[W] = [W]_0$ for all values of r at $t = 0$. The boundary conditions are easily written and are incorporated in Table IV.

The equations in Table IV can be integrated along with the equations for the apparent rate constants (Table II) for a given set of parameter values, using the finite-difference technique (11 grid points) in the radial direction and Gear's technique.[23] The intrinsic rate constants, $k_{i,0}$, are assumed to be of the following form:[10]

$$k_{i,0} = \zeta_i \lambda_0 \qquad i = 1, 2, 3 \qquad (17)$$

where ζ_1, ζ_2, and ζ_3 are the parameters (functions of temperature) that are curve fitted in this study. The dependence of $k_{i,0}$ on the concentration, λ_0, of the acid end groups at any location is assumed for the SSP of nylon 6 because it is well known[12] that these groups exert a catalytic effect in *melt* polymerization of ε-caprolactam, and a similar effect *could* be present in SSP as well. However, we have also carried out optimal parameter estimation studies assuming constant values of $k_{i,0}$:

$$k_{i,0} = \zeta_i \qquad i = 1, 2, 3 \qquad (18)$$

The equilibrium constants for the three reactions in Table I are assumed to be the same as those for melt polymerization.[12] Thus, the intrinsic rate constants for the reverse reactions are given by

$$k'_{i,0} = \frac{k_{i,0}}{K_i} \qquad i = 1, 2, 3 \tag{19}$$

Since there are no diffusional limitations for the forward and reverse steps of the ring opening reaction, as well as for the backward step of the polyaddition reaction, we have

$$k_1 = k_{1,0} \tag{20a}$$

$$k'_1 = k'_{1,0} \tag{20b}$$

$$k'_3 = k'_{3,0} \tag{20c}$$

The parameters θ_1, θ_2, and θ_3 have been assumed as curve-fit parameters in this study (along with ζ_i, $i = 1, 2, 3$). It may be added that Achilias and Kiparissides[13,14] have suggested the use of the theory of excess chain end mobility[24,25] for estimating these parameters. However, they were forced to introduce a curve-fit parameter, $j_{c,0}$, in this theory to obtain good agreement with experimental data on the isothermal polymerization of methyl methacrylate (MMA). Since a curve-fit parameter is necessarily to be used, we decided to use it for the entire group of variables clubbed together in the $\theta_i s$. A similar procedure was found to be successful in our recent work[26] on the modeling of MMA polymerization in semibatch reactors.

The macro-level diffusivity, $\mathbb{D}_w$, of water through the reaction mass is an important physical parameter in this work. Strictly speaking, $\mathbb{D}_w$ would be expected to decrease with the degree of crystallinity, and so would be a function of the reaction time, since the polymer crystallinity increases as its molecular weight increases. Also, the nonuniform molecular weight profile within the polymerizing particle would imply that the crystallinity would be a function of the distance from the surface of the particle. Thus, the diffusivity is not only time-dependent, but also position-dependent. In this study, however, we have assumed $\mathbb{D}_w$ to be constant at an average value. From the available data[27] on the diffusivity of water through nylon 6 at a few temperatures, we estimated $\mathbb{D}_w$ at the reaction temperature (190°C) to be 10^{-8} m^2/h. Use of this value does not give a good match with experimental results. This value is much too high. On closer scrutiny, it was found that the sample (film) of nylon 6 used to generate the correlation for $\mathbb{D}_w$ had a crystallinity of around 30%.[28] Gaymans et al.[5] have not provided any information on the crystallinity of the samples they used for generating experimental results on the SSP of nylon 6. We guess that the crystallinity of their samples (molecular weights around 20,000–30,000) could be as high as 75%. This would imply that $\mathbb{D}_w$ would be much lower than the value of 10^{-8} m^2/h predicted using the correlation in Ref. 27. Because of this uncertainty, we decided to treat $\mathbb{D}_w$ as a parameter in this simulation, alongwith ζ_i and θ_i ($i = 1, 2, 3$).

In order to obtain the initial conditions to simulate the SSP at 463 K for which some experimental data[5] are available in the open literature, we first simulated the *previous stage*, namely, melt polymerization[12] of ε-caprolactam using $[W]_0 = 0.16$ mol/kg, $[C_1]_0 = 8.8$ mol/kg, $T = 513$ K, until a desired value of the number-average chain length, μ_n, was obtained. This provided values for all the concentrations and moments at the end of the liquid phase polymerization. These values were taken to be the starting values (at $t = 0$) for the SSP, except for the concentrations of ε-caprolactam and water. $[C_1]$ and $[W]$ at $t = 0$ for the SSP, were taken as zero to duplicate their extraction out of the pellets produced experimentally by Gaymans et al.[5] from melt-polymerized nylon 6. The starting concentrations used for simulation of SSP of nylon 6 are listed in Table V for their different experimental runs[5] (corresponding to different values of the initial number-average chain length, $\mu_{n,0}$). It must be emphasized that the complete details on the conditions used by Gaymans et al.[5] for producing the initial samples for SSP are not available in their study, and this is why we have tried to generate initial values using the above technique, trying to match the only variable ($\mu_{n,0}$) whose value is mentioned.

An optimal parameter estimation computer program has been used to obtain the best-fit values of the seven parameters (ζ_i, θ_i; $i = 1, 2, 3$; $\mathbb{D}_w$) using the isothermal experimental data on nylon 6 SSP. The Box complex algorithm[29,30] has been used for this purpose. The objective function that has been optimized in the program is

$$F(\zeta_i, \theta_i; i = 1, 2, 3; \mathbb{D}_w) = \max\left[-\sum_{j=1}^{N} \frac{\text{abs}\{\mu_{n,\text{exptl}}(j) - \mu_{n,\text{theor}}(j)\}}{\mu_{n,\text{theor}}(j)}\right] \tag{21}$$

where N is the total number of experimental data points for *all* $\mu_{n,0}$ reported,[5] and the subscripts, exptl and theor, indicate the experimental and theoretical values of μ_n.

RESULTS AND DISCUSSION

The computer program was tested for several special cases to ensure that it was free of errors. The number

Table V Starting Concentrations for SSP[a]

	Initial Concentrations (mol/kg) for Different Runs of SSP				
	$\mu_{n,0}$ = 22	35	55	72	95
$[C_1]$	0.0000	0.0000	0.0000	0.0000	0.0000
$[P_1]$	0.00075	0.00068	0.0006	0.00055	0.00049
λ_0	0.03122	0.04331	0.05244	0.05456	0.05367
λ_1	0.69388	1.53307	2.93076	3.95800	5.13901
λ_2	22.10	80.43	260.10	485.20	902.20
$[W]$	0.0000	0.0000	0.0000	0.0000	0.0000

[a] Initial conditions in liquid phase polymerization to obtain the above values:

Temperature = 513.0 K
$[C_1]_0$ = 8.8 mol/kg
$[P_1]_0$ = 0.0 mol/kg
$\lambda_{0,0}$ = 0.0 mol/kg
$\lambda_{1,0}$ = 0.0 mol/kg
$\lambda_{2,0}$ = 0.0 mol/kg
$[W]_0$ = 0.16 mol/kg

of finite-difference grid points was increased from 11 to 21 and the results on $\bar{\mu}_n(t)$ were found to be essentially the same (within 1% at t = 24 h). Similarly, the results were unaffected when the parameter, TOL, in the NAG library subroutine, D02EBF, was decreased from 10^{-4} to 10^{-8}. After these tests, the Box complex method was used to obtain the best-fit values of the seven curve-fit parameters, using both Eqs. (17) and (18) for $k_{i,0}$. Table VI gives the final values of these parameters for both these cases.

Simulation results for the five different experimental runs[5] (corresponding to different values of the initial number-average chain length, $\mu_{n,0}$) using the best-fit values of the parameters (Table VI) are shown by the solid curves in Figures 2 and 3 for the case when the intrinsic rate constants, $k_{i,0}$, are proportional to the zeroth moment [Eq. (17)]. The experimental data points are also shown in these diagrams. Excellent agreement between theory and experimental data is observed. The dotted curves in these diagrams show the theoretical results using the best-fit values of the parameters with $k_{i,0} = \zeta_i$ [Eq. (18)]. The final values of the objective function, F [in Eq. (21)], for these two choices of $k_{i,0}$ are −2.53 and −1.89, respectively. Based on these values as well as on the agreement between the theoretical curves and experimental data in Figures 2 and 3, it is difficult to say which of these two cor-

Table VI Best-Fit Values of the Parameters Used for the Simulation of SSP of Nylon 6 at 190°C

	For $k_{i,0} = \zeta_i \lambda_0$	For $k_{i,0} = \zeta_i$
Optimal parameters		
θ_1 (h)	4.626×10^{-4}	3.339×10^{-4}
θ_2 (h)	406.557	486.251
θ_3 (h)	6476.71	2586.66
ζ_1	49.183 (kg^2 mol^{-2} h^{-1})	0.3247 (kg mol^{-1} h^{-1})
ζ_2	14996.9 (kg^2 mol^{-2} h^{-1})	405.7 (kg mol^{-1} h^{-1})
ζ_3	360.59 (kg^2 mol^{-2} h^{-1})	7.7116 (kg mol^{-1} h^{-1})
$\mathbb{D}_w$ (m^2/h)	3.366×10^{-11}	1.065×10^{-11}
Other parameters/conditions		
$R = 2 \times 10^{-4}$ m		
$[W]_s$ = 0.00001 mol/kg		
T = 463 K		

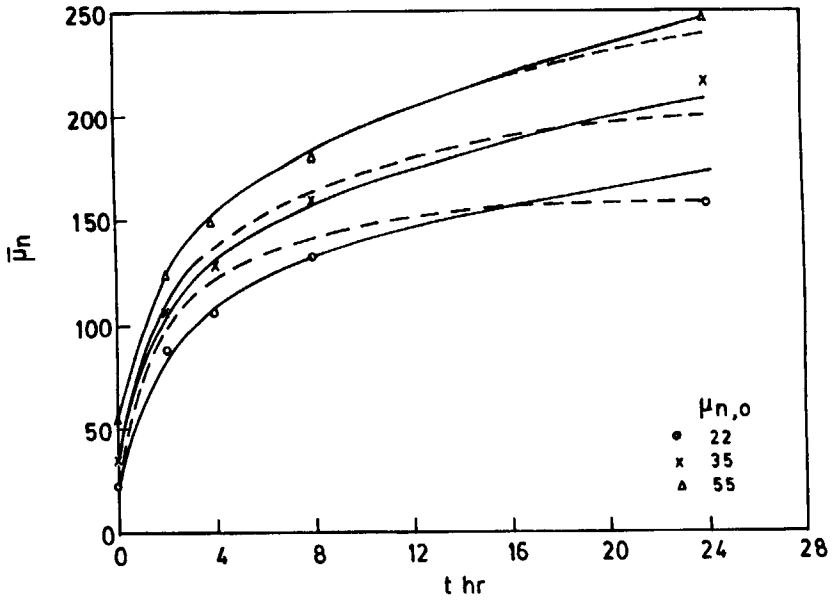

Figure 2 Comparison of simulation results with experimental data at 190°C for $\mu_{n,0} = 22$, 35, 55. Reference values of the parameters (Table VI) used. Equations (17) ($k_{i,0} = \zeta_i \lambda_0$, solid) and (18) ($k_{i,0} = \zeta_i$, dotted) used for $k_{i,0}$.

relations for the intrinsic rate constants is superior, and we have arbitrarily selected the form in Eq. (17) for further study in this work. A comparison of the present results with those from our earlier work,[10] which used the Fujita–Doolittle theory for the micro-level diffusivity reveals that the agreement of the

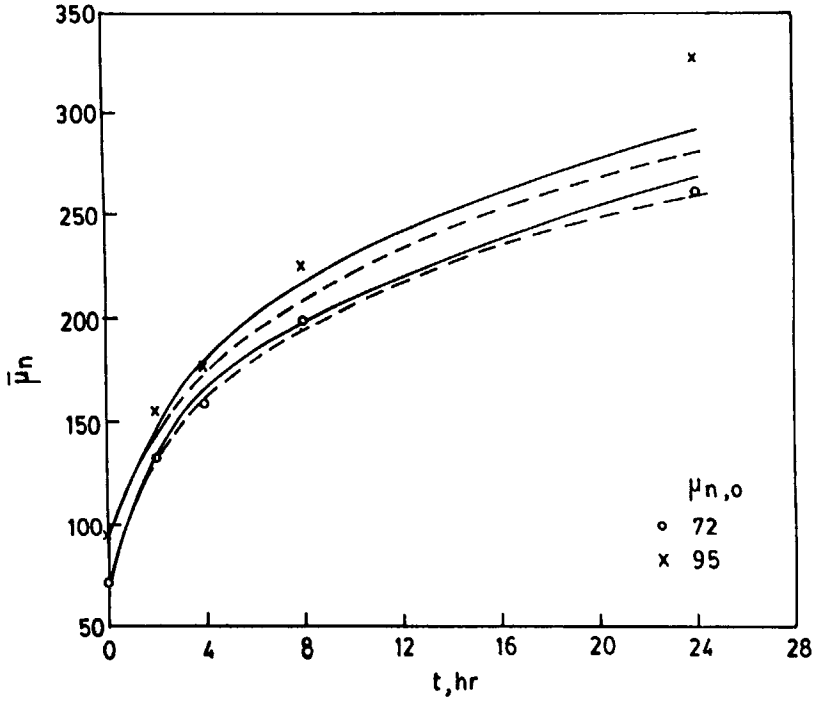

Figure 3 Comparison of simulation results with experimental data at 190°C for $\mu_{n,0} = 72$, 95. Reference values of the parameters (Table VI) used. Same notation as in Fig. 2.

present theory is better. In addition, the present theory is more elegant since the parameters of the Vrentas–Duda theory are obtained by independent measurements on nonreacting systems.

The sensitivity of the results to the parameters is now studied [using Eq. (17) for $k_{i,0}$]. The value of $\mu_{n,0}$ of 55 is selected for this purpose. Figures 4–8 show the effects of varying the seven different parameters one by one, about their best-fit values, keeping the other parameters at their reference (Table VI) values. The effect of θ_1 on $\bar{\mu}_n$ is shown in Figure 4. Decreasing θ_1 speeds up the reaction, particularly in the initial stages, and increases the final values of $\bar{\mu}_n$. Lower values of θ_1 signify higher values of the micro-level diffusivity of the polymer molecule in the reaction mass. This leads to an increase in the forward rate constant of the polycondensation reaction (other quantities remaining unchanged) and hence in the values of $\bar{\mu}_n$. Very high values of θ_1 (> 0.01 h) suppress the forward step of the polycondensation reaction so much that depolymerization takes place during the early stages. It is interesting to note that this figure illustrates how the presence of diffusional limitations (nonzero values of θ_1) reduces the value of $\bar{\mu}_n$ significantly.

The effect of varying the parameter, θ_2, on the progress of reaction is shown in Figure 5. Increased values of θ_2 lead to a decrease in the micro-level diffusivity of the water molecule and a corresponding decrease in the reverse rate constant, k'_2 (other quantities remaining unchanged). This means that the polycondensation reaction is forced toward the right, leading to higher values of $\bar{\mu}_n$. The sensitivity of the results to θ_2 is less than that toward θ_1.

The results are found to be relatively insensitive to the value of θ_3. Decreasing θ_3 from the reference values of 6476.7 to 100 h decreases the value of $\bar{\mu}_n$ at $t = 24$ h only from about 246.1 to 220.65. A similar insensitivity of $\bar{\mu}_n$ is observed to the value of ζ_1 (between 10 and 1000 h). In fact, use of $\zeta_1 = 0$ (which makes $k'_{1,0} = 0$) also gave the same $\bar{\mu}_n$ history. This means that the ring opening reaction in Table I can easily be omitted. Indeed this reaction was omitted in our previous study,[10] based on intuitive reasoning. It may be emphasized that we cannot omit the polyaddition reaction from the kinetic scheme, even though we get the same results with $\theta_3 \rightarrow \infty$ (i.e., $k_3 = 0$). This is because the rate constant, $k'_{3,0}$ of the reverse step does not become zero as $\theta_3 \rightarrow \infty$. Indeed, this reverse reaction is responsible for increasing the value of $[C_1]$ in the polymer particle from its initial value of zero, as the polymerization progresses.

Figure 6 shows the effect of varying ζ_2. Increasing the value of ζ_2 beyond the reference value of 14996.9–22000 kg^2 mol^{-1} h^{-1} does not affect the progress of

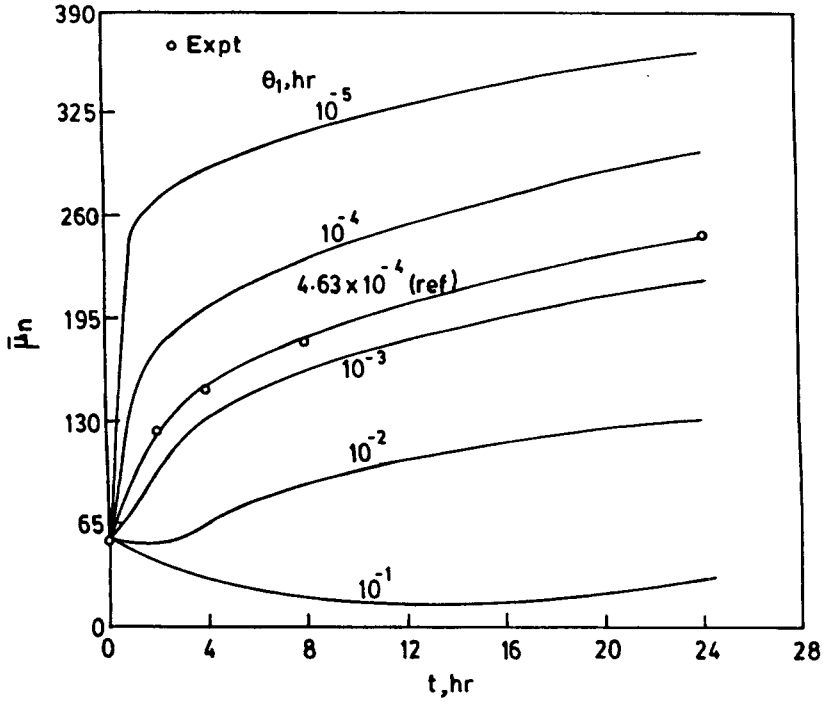

Figure 4 Effect of θ_1 on $\bar{\mu}_n$. $T = 190$°C, $\mu_{n,0} = 55$, $k_{i,0} = \zeta_i \lambda_0$ [Eq. (17)]. Reference values of the other parameters (Table VI) used.

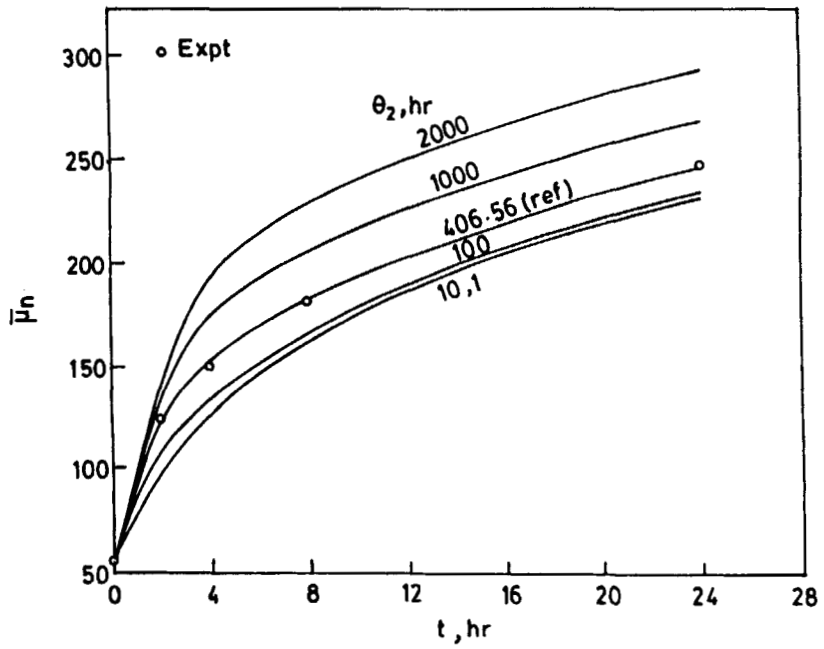

Figure 5 Effect of θ_2 on $\bar{\mu}_n$. Reference values of the other parameters used.

the reaction much, but lowering the values of ζ_2 does lead to considerable effect on the progress of the reaction. In fact, it is observed that as ζ_2 is increased from a low value of 100–22000 $kg^2\ mol^{-1}\ h^{-1}$, $\bar{\mu}_n(t)$ goes up with time more rapidly near $t \simeq 0$ (due to higher rates of the forward step in the polycondensation reaction), but flattens out at larger values of t to give lower final values of $\bar{\mu}_n$. The latter is

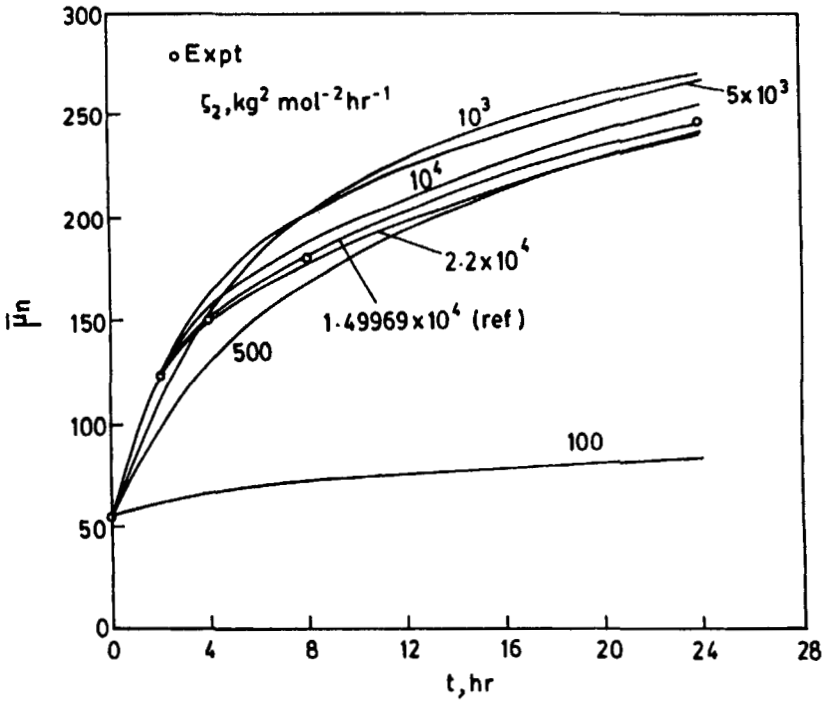

Figure 6 Effect of ζ_2 on $\bar{\mu}_n$. Reference values of other parameters used.

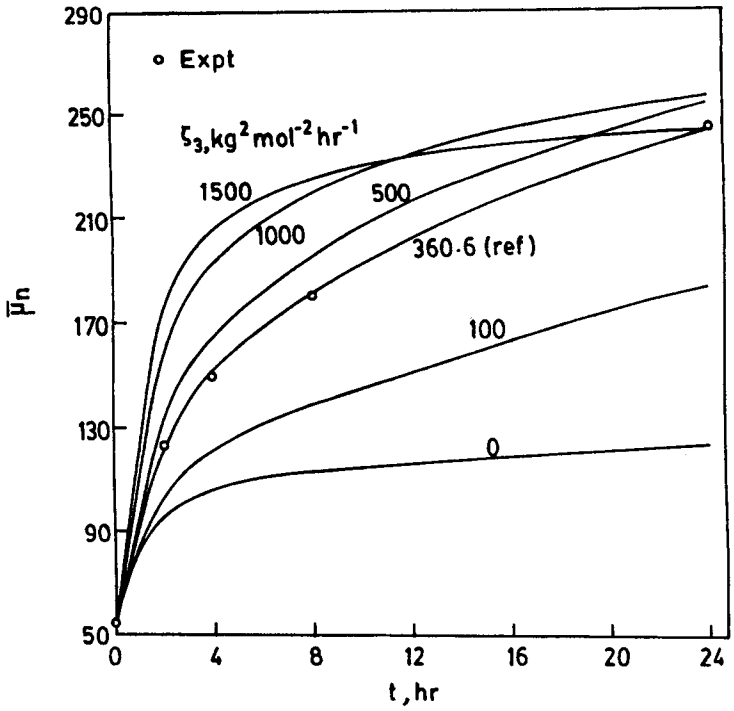

Figure 7 Effect of ζ_3 on $\bar{\mu}_n$. Reference values of other parameters used.

because diffusional limitations become more pronounced and occur earlier for higher values of ζ_2. Figure 6, thus, illustrates the effect of competing physical phenomena. A similar phenomenon is observed in Figure 7, where ζ_3 is varied (note ζ_3 going from 500 to 1500 kg^2 mol^{-2} h^{-1}). The curve for $\zeta_3 = 0$ (which makes $k'_{3,0} = 0$ also) in Figure 7 shows what happens when we omit the polyaddition reaction from our kinetic scheme. This behavior is to be contrasted with the curve for $\xi_2 = 100$ kg^2 mol^{-1} h^{-1} in Figure 6. The importance of the polycondensation reaction over the polyaddition reaction is quite evident.

The macro-level diffusivity of water through the reaction mass, $\mathbb{D}_w$ (or the degree of crystallinity), plays an important role in SSP as shown in Figure 8. For values of $\mathbb{D}_w$ above about 10^{-10} m^2/h (corresponding to higher fractions of amorphous material), the values of $\bar{\mu}_n$ are higher. Values of $\mathbb{D}_w$ below the reference value of 3.37×10^{-11} m^2/h lead to lower $\bar{\mu}_n$. The results become relatively insensitive to $\mathbb{D}_w$ below a value of about 10^{-13} m^2/h. For such cases, the water produced by chemical reaction does not diffuse out much, and the reaction is driven toward final values of $\bar{\mu}_n$ controlled by equilibrium alone. One need not solve partial differential equations for such cases. It should be emphasized that the degree of crystallinity would affect not only $\mathbb{D}_w$ but also the values of θ_i, and its influence would be more than depicted by Figure 8.

The effect of varying some important *operating* conditions has also been studied. The increase in $\bar{\mu}_n$ is found to be relatively insensitive to the surface concentration of water, $[W]_s$, when its value is below about 10^{-3} mol/kg (see Fig. 9). For values of $[W]_s$ above about 10^{-3} mol/kg, however, the results are found to be sensitive to its value. This implies, technologically, that one needs to reduce the concentration of water in the vapor phase surrounding the nylon 6 to a threshold value, and not much is achieved in going below this level. It is interesting to note that the difference in $[W]_s$ shows up only after about 6 h of SSP. The radius, R, of the nylon 6 powder (assumed spherical) is within the range of 0.2–0.5 mm, as reported by Gaymans et al.[5] The reference value used in this study is 0.2 mm. It is found that (see Fig. 10) decrease in the value of R from 0.5 to 0.2 mm causes an increase in the final value of $\bar{\mu}_n$ of about 40–50. It is interesting to note that much more is achieved by reducing the pellet size from 0.3 to 0.2 mm than from 0.5 to 0.4 mm. This is because the major part of polymerization occurs in a thin shell near the periphery (see later). Figures 9 and 10 quantify the effect of two of the most important operating conditions.

We also carried out a simulation run for the case

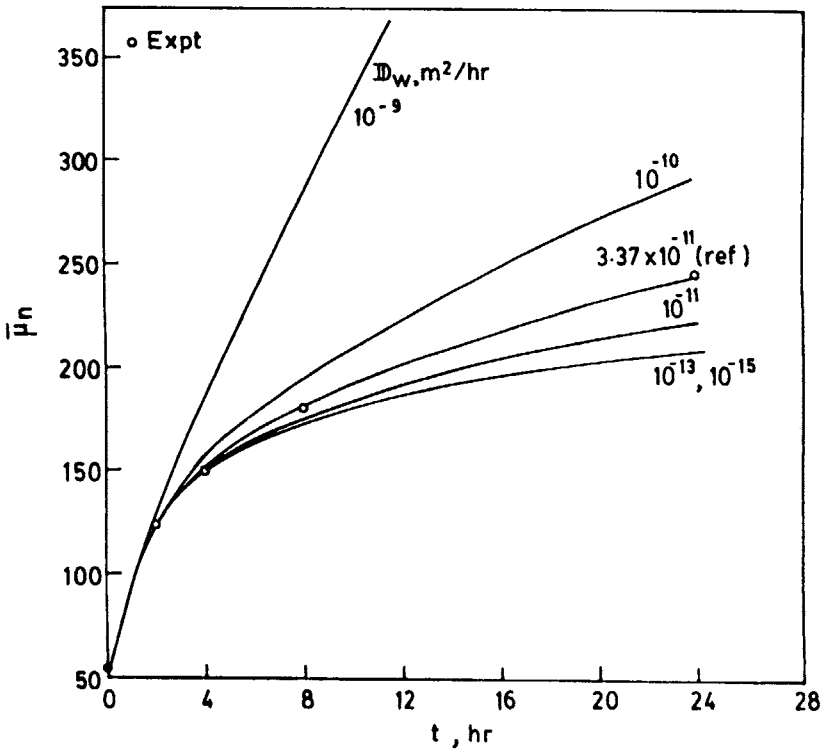

Figure 8 Effect of the $\mathbb{D}_w$ on $\bar{\mu}_n$. Reference values of other parameters used.

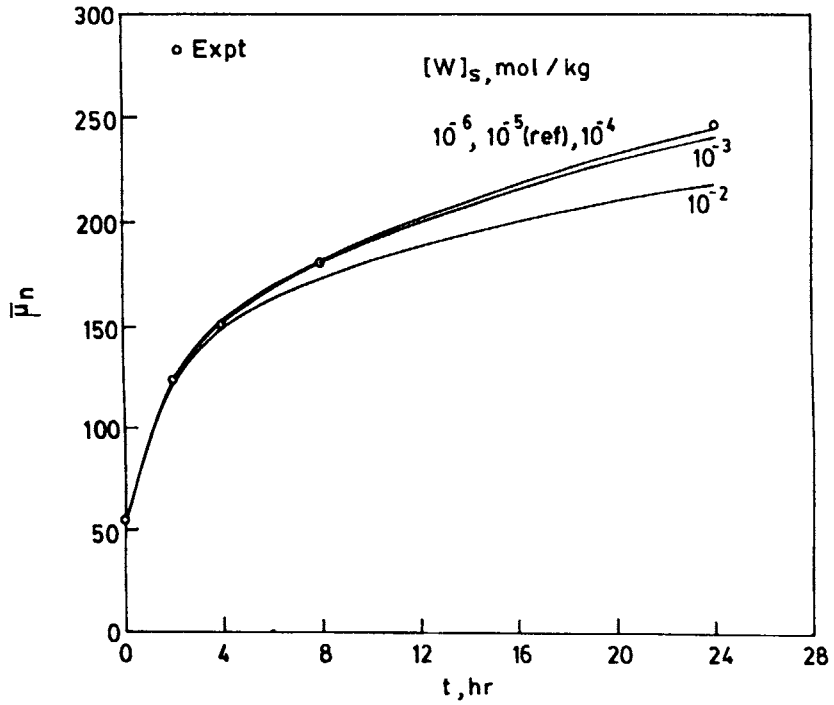

Figure 9 Variation of $\bar{\mu}_n$ with time as $[W]_s$ is changed. Reference values of all parameters used.

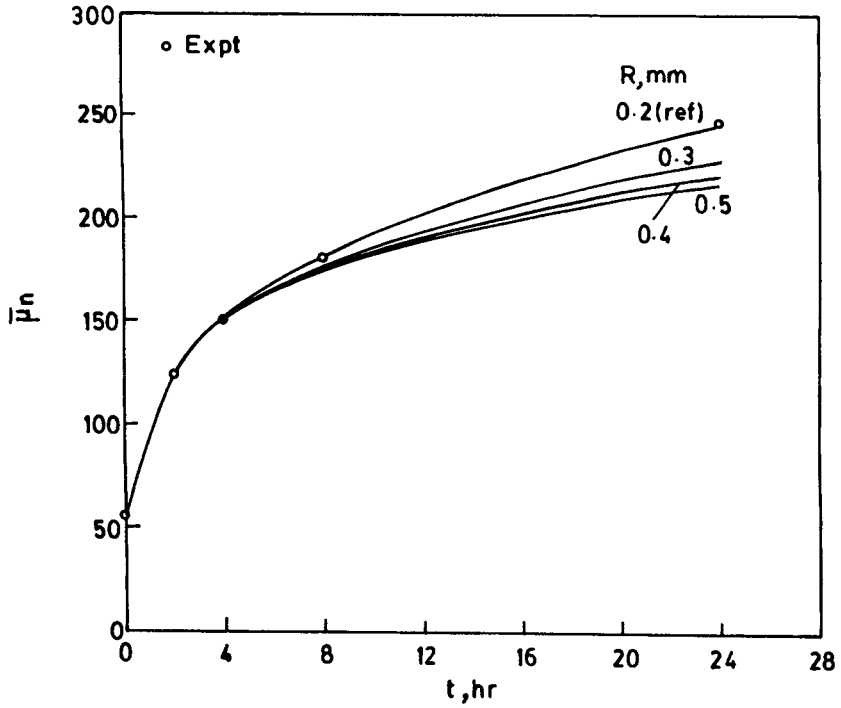

Figure 10 Variation of $\bar{\mu}_n$ with time as R is changed. All other conditions are the same as for the reference run.

when the monomer and water are not leached out of the polymer particles before the SSP, using the reference values of all the parameters (for the case when $k_{i,0} = \zeta_i \lambda_0$). The values of $[C_1]_0$ and $[W]_0$ are 5.869 and 0.09683 mol/kg, respectively (for $\mu_{n,0} = 55$). A sudden jump in $\bar{\mu}_n$ is observed near $t \sim 0$, but the values for t larger than about 9 h are much lower (213.7 as compared to 246.1 at $t = 24$ h). The sharp initial rise in $\bar{\mu}_n$ is due to high initial concentration of the monomer, which drives the polyaddition reaction to the right-hand side. This effect dominates over the effect of higher $[W]$ values, which drives the polycondensation reaction to the left (depolymerization). The lower final values of $\bar{\mu}_n$ emphasizes the need for carrying out leaching before SSP.

Figure 11 shows the results for SSP of nylon 6 with a single intermediate remelting (homogenizing) of the polymer particles. Reference values (Table VI) of the parameters have been used. Points p, q, r, and s in this figure show that if the total time for SSP (i.e., before and after remelting) is the same (24 h), higher $\bar{\mu}_n$ product can be obtained by intermediate and early homogenization. The results are not as dramatic if the homogenization occurs late. This trend is qualitatively similar to the experimental observations of Gaymans et al.[5] The higher values of $\bar{\mu}_n$ result from lower (uniform) values of $[W]$ in the inside of the polymer particles, resulting from homogenization.

Figure 12 shows the water concentration profiles at different values of t (in absence of remelting) for the reference conditions. It is observed that the water concentration builds up in the interior of the polymer particle (due to generation) quite early during the reaction. However, macro-level diffusion of W leads to a relatively sharp decrease in $[W]$ in the outer shell of the particle, 0.16 mm $< r <$ 0.2 mm. The lower water concentrations in the outer shell are associated with significantly higher values of μ_n in this region, as shown in Figure 13. This also explains why remelting of the polymer particle leads to higher $\bar{\mu}_n$ product, as shown in Figure 11, since intermediate homogenization removes the spatial gradient and reduces the averaged value of $[W]$ in the inner regions. It may be added that these profiles have been generated using 21 finite-difference grid points because of the relatively sharp gradients near $r = R$.

Figure 14 shows how the monomer concentration increases from its initial value of zero as the reaction progresses. Since it has already been found that the ring opening reaction is unimportant, this means that the reverse step of the polyaddition reaction is

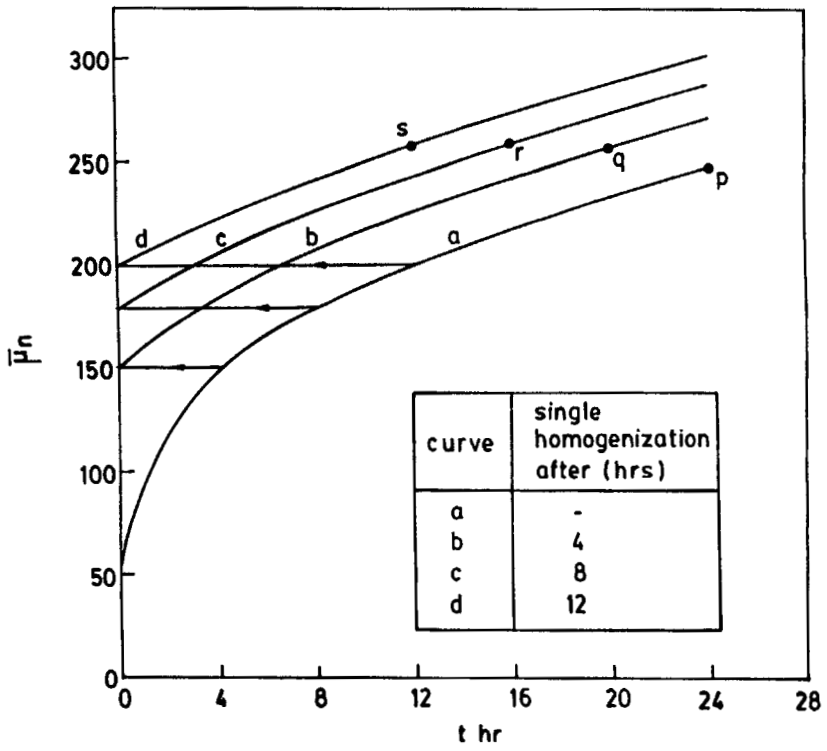

Figure 11 Comparison of the results for SSP with single intermediate homogenization (remelting) of polymer sample. Curve *a* is the reference run.

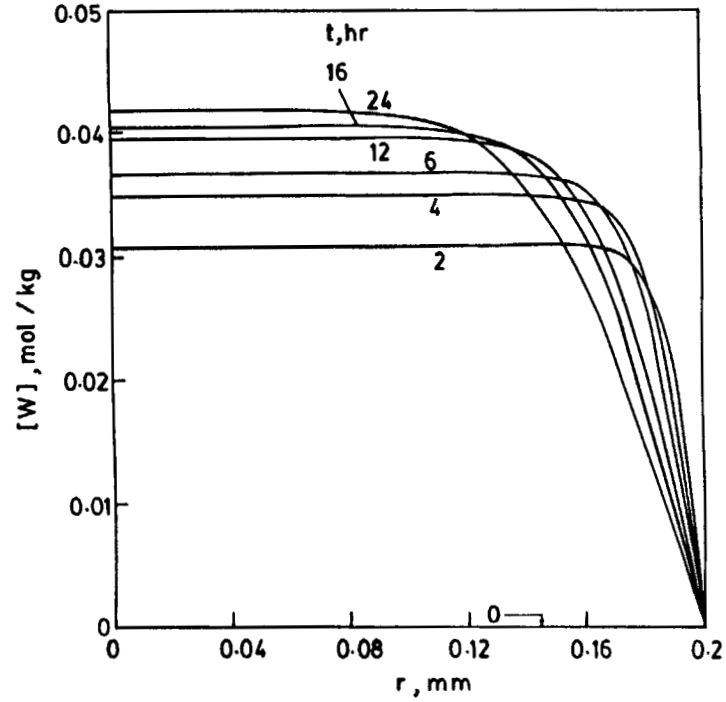

Figure 12 Radial profile of $[W]$ at different times for the reference run [with $\mu_{n,0} = 55$ and with Eq. (17)].

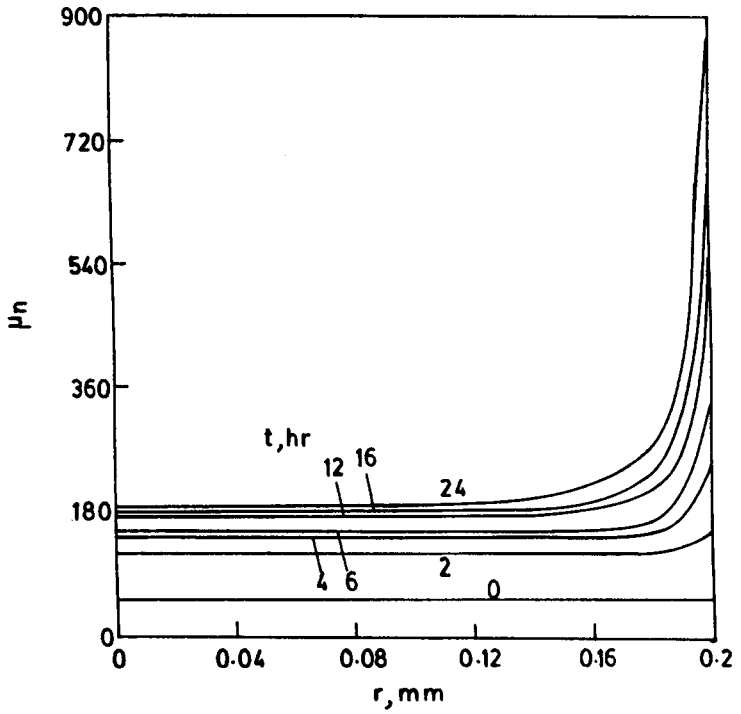

Figure 13 Radial profile of μ_n at different times for the reference run.

responsible for the generation of the monomer. The reason why $[C_1]$ is lower near the outer fringes of the polymer particle is because the total concentration of polymer (i.e., $\Sigma\ [P_n]$) molecules is lower there (associated with the higher values of μ_n).

The variation of μ_n with location would be ex-

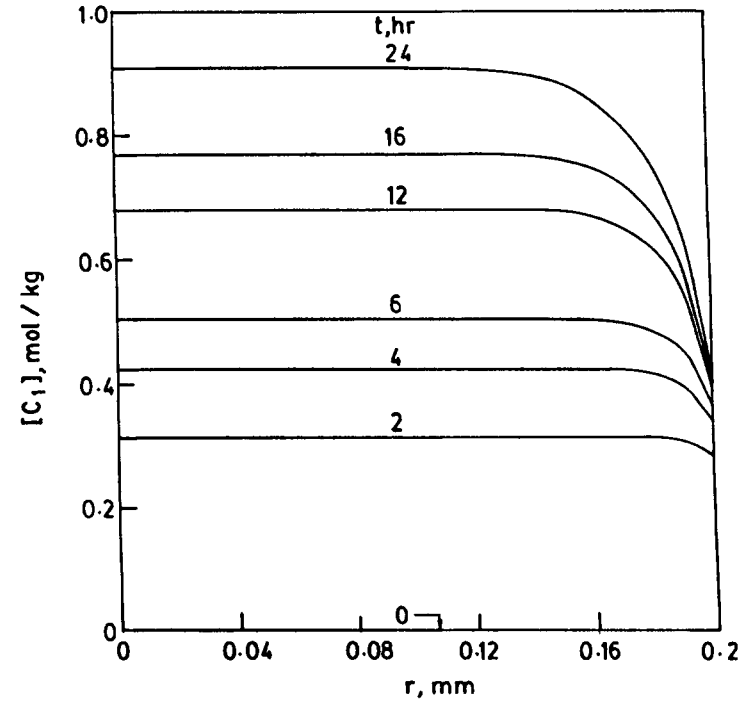

Figure 14 Radial profile of $[C_1]$ at different times for the reference run.

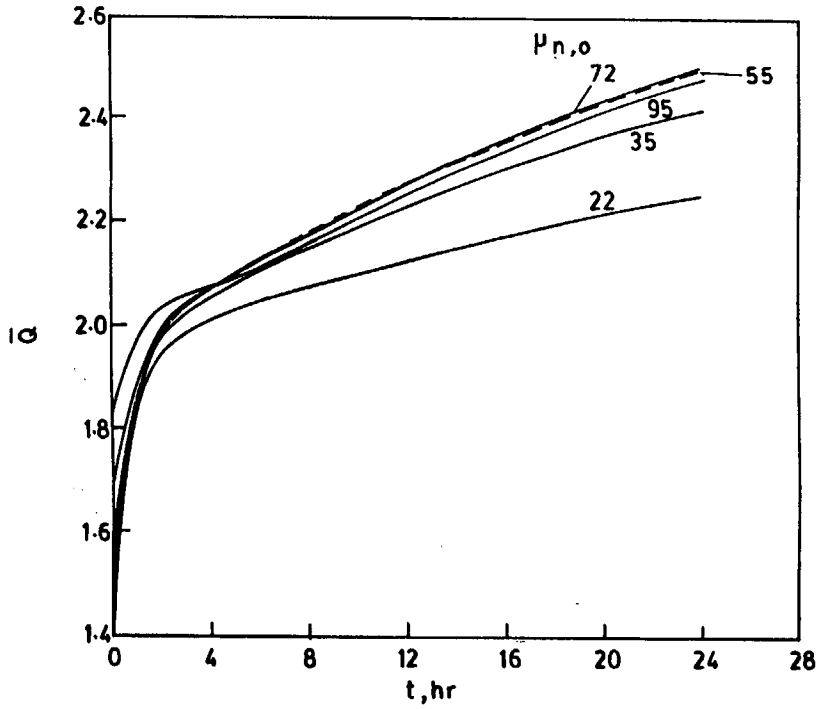

Figure 15 Variation of average polydispersity index, $\bar{Q}$, with time for $\mu_{n,0}$ = 22, 55, 72, 95. Equation (17) used for $k_{i,0}$. Reference values of all parameters used.

pected to lead to values of the spatially averaged (mixed) polydispersity index, $\bar{Q}$, above the normal value of 2.0. Figure 15 shows how $\bar{Q}$ increases with time for the five cases studied. $\bar{Q}$ is found to rise rapidly at first, and then increases more gradually to values above 2.0. The initial values of $\bar{Q}$ are not 2.0 for the low $\mu_{n,0}$ cases due to low conversions at the beginning.

It is interesting to note (see Fig. 16) that the apparent rate constant, k_2, *increases* with time, rather than decreases. This diagram shows k_2 at two positions, one near the center of the spherical polymer particle (at r = 0.04 mm) and the other near the periphery (at r = 0.18 mm) for the reference run (with $\mu_{n,0}$ = 55). The value of the intrinsic rate constant, $k_{2,0}$, is found to decrease with time at both these locations. The latter is associated with a drop in the value of λ_0 [see Eq. (17)], which, in turn, is due to the increase in the value of μ_n with time. Figure 13 shows that μ_n is higher at r = 0.18 mm, and so λ_0 and $k_{2,0}$ would be expected to be lower at this location than at r = 0.04 mm. This is indeed confirmed in Figure 16. Figure 17 shows that the ratio, $k_2/k_{2,0}$, increases with time at both locations. This increase indicates that the diffusional resistance *decreases* as the SSP progresses. This behavior is in sharp contrast to the increase in the diffusional resistance in the polymerization of MMA (gel effect). The decreasing diffusional resistance in the SSP of nylon 6 is associated with the decrease in the volume fraction, ϕ_p, of the polymer with time due to generation of C_1 and W. In fact, Figs. 12, 14, and 17 show that as t increases, $[C_1]$ increases at both locations but $[W]$ increases continuously at r = 0.04 mm only ($[W]$ decreases with time at r = 0.18 mm after an initial rise). This leads to ϕ_p being higher at r = 0.18 mm. This complex interplay of several phenomena—generation of C_1 and W, the macro-diffusion of W, decrease of λ_0 and $k_{2,0}$ with polymerization, etc.—in influencing the rate constant, k_2, is clearly brought out in these figures. Similar increases in $k_3/k_{3,0}$ and $k_2'/k_{2,0}'$ with time are also observed.

It may be mentioned here that most of the simulation results reported herein have been generated using the closure conditions given in Table IV. Use of $[P_2] = [P_1]$ gives negative monomer concentrations for *some* extreme choices of parameters *which are far removed from the reference values,* e.g., for very low ζ_1 and very high ζ_3. Whenever this is encountered, we have used the closure condition, $[P_2] = 0.001\,[P_1]$. The moment closure equation in Table IV is used unchanged. Results were regenerated using this new closure equation for all the other pa-

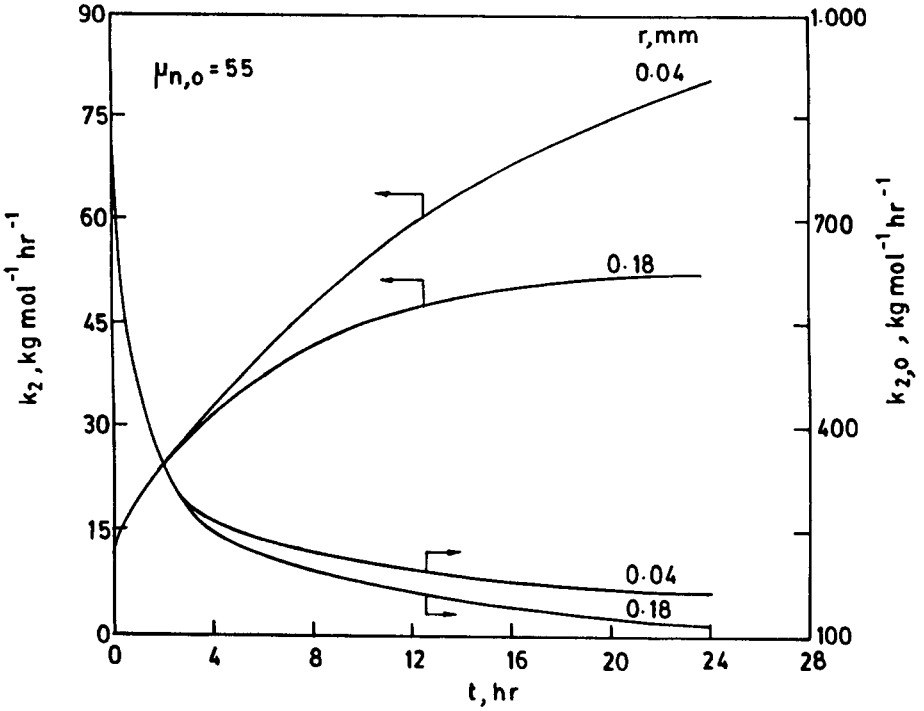

Figure 16 Variation of k_2 and $k_{2,0}$ with time at two radial positions (r = 0.04, 0.18 mm) for the reference run.

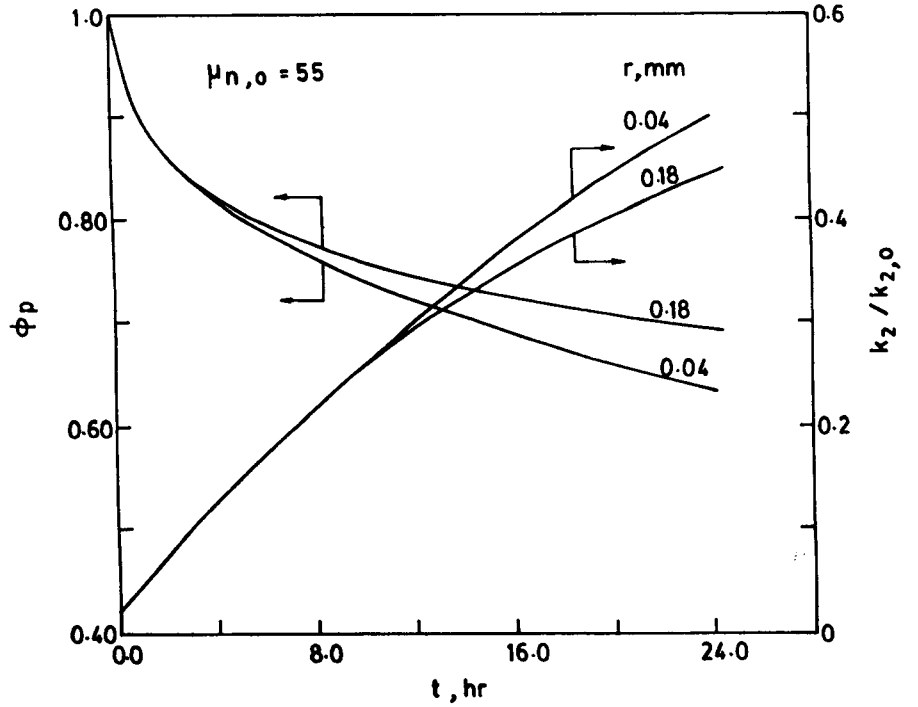

Figure 17 Variation of ϕ_p and $k_2/k_{2,0}$ with time at two radial positions (r = 0.04, 0.18 mm) for the reference run.

rameter values too and were found to be insensitive to this change. We recommend the use of this new closure condition in future studies.

CONCLUSIONS

A new model having a strong molecular basis has been proposed to account for the effects of segmental diffusion on reversible step growth polymerizations. This model is more fundamental and general than earlier models on SSP and can be used to analyze a variety of SSP processes, as for example, nylon 6, polyethylene terephthalate, polybutylene terephthalate, nylon 66, etc. The model is applied to the specific case of the SSP of nylon 6 in this study. A comparison of the present results with our earlier work[10] reveals that agreement of this theory with available experimental data at 190°C is far better.

The optimal values of six parameters, ζ_i and θ_i; $i = 1, 2, 3$ (or five, with $\zeta_1 = 0$ and $\theta_3 \to \infty$) obtained in this study can be used at 190°C (along with the model equations and the new closure condition developed in this work) to design and optimize industrial nylon 6 SSP reactors in the future. The seventh parameter, $\mathbb{D}_w$, used in this study depends on the crystallinity of the sample, and must be estimated using pilot plant studies, till such time that a better understanding relating it to the morphology (which could be independently studied) becomes available. It may be added that similar optimal-parameter estimation could be performed for SSP of other polymers (or for nylon 6 at other temperatures), to give a more rational design methodology for those reactors as well. This study quantifies the effects of three important operation parameters, namely, radius of the polymer particle, water concentration in the vapor phase, and the degree of crystallinity of nylon 6 on the spatially averaged molecular weight history.

NOMENCLATURE

–A	Polymer molecule with an unreacted A group
–B	Polymer molecule with an unreacted B group
C_1	ε-Caprolactam
D_m, D_p, D_s	Overall (micro-level) diffusivity of monomer, polymer, solvent molecule, respectively, m^2/h.
$D_{m,\mathrm{ref}}$, $D_{p,\mathrm{ref}}$, $D_{s,\mathrm{ref}}$	Overall diffusivity of monomer, polymer and solvent molecule at reference condition, m^2/hr.
$\mathbb{D}_w$	Diffusivity (macro-level) of water inside the reacting pellet, m^2/h.
k_i	Overall forward rate constant of ith reaction in the solid phase, kg mol^{-1} h^{-1}.
k'_i	Overall reverse rate constant of ith reaction in the solid phase, kg mol^{-1} h^{-1} or h^{-1}.
$k_{i,0}$	Intrinsic forward rate constant of ith reaction in the solid phase, kg mol^{-1} h^{-1}.
$k'_{i,0}$	Intrinsic reverse rate constant for ith reaction in the solid phase ($=k_{i,0}/K_i$), kg mol^{-1} h^{-1} or h^{-1}
K_i	Equilibrium constant of ith reaction.
K_s	Parameter in equation for glass transition temperature of polymer, K^{-1}
(MW_m), (MW_s)	Molecular weights of pure monomer and solvent, kg mol^{-1}
M_{jp}	Molecular weight of jumping polymer unit, kg mol^{-1}
P_n	Polymer molecule of chain length n.
$[P]$	Concentration of polymer molecules P of all lengths, mol/kg
$\bar{Q}$	Spatially averaged polydispersity index $\equiv (\bar{\lambda}_2/\bar{\lambda}_1)/(\bar{\lambda}_1/\bar{\lambda}_0)$
r_D	Radius at which the concentration of polymer molecule P approaches the bulk value, m
$r_{m,j}$	Radius swept by a polymer molecule having one unreacted A group fixed at one end, m
R	Radius of the solid pellet, m
T	Reaction temperature, K
T_g	Glass transition temperature, K
$T_{g\infty}$	Glass transition temperature at infinite chain length, K.
$\hat{V}^*_m$, $\hat{V}^*_p$, $\hat{V}^*_s$	Specific critical hole free volume of monomer, polymer, or solvent, m^3/kg
$\hat{V}^0_m$, $\hat{V}^0_p$, $\hat{V}^0_s$	Specific volumes of monomer, polymer, or solvent, m^3/kg
V_{fm}, V_{fs}, V_{fp}	Free volume fraction of monomer, solvent, and polymer, respectively, inside the reacting pellet.
$[W]_s$	Surface concentration of water, mol/kg

Greek Letters

α_g Coefficient of thermal expansion of polymer in glassy state, K^{-1}

α_l Coefficient of thermal expansion of polymer in liquid state, K^{-1}

γ Overlap factor

$\theta_1, \theta_2, \theta_3$ Adjustable parameters in the model, h

λ_k kth moment of all polymer molecules, $\lambda_k = \sum_{n=1}^{\infty} n^k[P_n]; k = 0, 1, 2, \ldots,$ mol/kg

$\bar{\lambda}_k$ Spatial-average value of λ_k $= \dfrac{\int_0^R r^2 \lambda_k \, dr}{\int_0^R r^2 \, dr}$

μ_n Number-average chain length $\equiv \lambda_1/\lambda_0$

$\bar{\mu}_n$ Spatial-average value of μ_n $= \dfrac{\int_0^R r^2 \lambda_1 \, dr}{\int_0^R r^2 \lambda_0 \, dr} \equiv \dfrac{\bar{\lambda}_1}{\bar{\lambda}_0}$

ζ_j Parameter used in the forward rate constant for the jth reaction in solid phase, $kg^2\ mol^{-2}\ h^{-1}$.

ξ_{13}, ξ_{23} Ratio of volume of a monomer (or solvent) molecule to the volume of a polymer jumping unit

ρ_m, ρ_p, ρ_s Density of pure (liquid) monomer, polymer, or solvent at temperature T (at time t), $kg\ m^{-3}$

ρ_m^0, ρ_s^0 Density of pure (liquid) monomer or solvent at initial temperature, $kg\ m^{-3}$

ϕ_m, ϕ_p, ϕ_s Volume fractions of monomer, polymer, or solvent in liquid at time t

χ as defined in Table II

Subscripts

b bulk value

m monomer (ε-caprolactam)

p polymer

s solvent (water)

REFERENCES

1. F. C. Chen, R. G. Griskey, and G. H. Beyer, *AIChEJ*, **15,** 680 (1969).
2. E. Schaff, H. Zimmerman, W. Dietzel, and P. Lohmann, *Acta Polym.*, **32,** 250 (1981).
3. T. M. Chang, *Polym. Eng. Sci.*, **10,** 364 (1970).
4. R. G. Griskey and B. I. Lee, *J. Appl. Polym. Sci.*, **10,** 105 (1966).
5. R. J. Gaymans, J. Amritharaj, and H. Kamp, *J. Appl. Polym. Sci.*, **27,** 2513 (1982).
6. F. Pilati, in *Comprehensive Polymer Science, Vol. 5: Step Polymerization,* G. C. Eastmond, A. Ledwith, S. Russo, and P. Sigwalt, Eds., Pergamon, New York, 1989, p. 201.
7. S. Fakirov, in *Solid State Behavior of Linear Polyesters and Polyamides,* J. M. Schultz and S. Fakirov, Eds., Prentice-Hall, Englewood Cliffs, N.J., 1990.
8. A. Kumar, K. Saksena, J. P. Foryt, and S. K. Gupta, *Polym. Eng. Sci.*, **27,** 753 (1987).
9. W. Y. Chiu, G. M. Carratt, and D. S. Soong, *Macromolecules,* **16,** 348 (1983).
10. A. Kaushik and S. K. Gupta, *J. Appl. Polym. Sci.*, **45,** 507 (1992).
11. J. S. Vrentas and J. L. Duda, *AIChEJ,* **25,** 1 (1979).
12. S. K. Gupta and A. Kumar, *Reaction Engineering of Step Growth Polymerization,* Plenum, New York, 1987.
13. D. Achilias and C. Kiparissides, *J. Appl. Polym. Sci.*, **35,** 1303 (1988).
14. D. S. Achilias and C. Kiparissides, *Macromolecules,* **25** (1994).
15. R. N. Haward, *J. Macromol. Sci., Rev. Macromol. Chem.*, **C4,** 191 (1970).
16. S. Sugden, *J. Chem. Soc.*, 1786 (1927).
17. D. W. van Krevelen, *Properties of Polymers,* 2nd ed., Elsevier, New York, 1974, pp. 410–421.
18. R. E. Kirk and D. F. Othmer, *Encyclopedia of Chemical Technology,* Vol. 24, 3rd ed., Wiley, New York, 1982, p. 280.
19. G. B. McKenna, in *Comprehensive Polymer Science, Vol. 2, Polymer Properties,* C. Booth and C. Price, Eds., Pergamon, New York, 1974.
20. J. M. Zielinski and J. L. Duda, *AIChEJ,* **38,** 405 (1992).
21. F. Bueche, *Physical Properties of Polymers,* Wiley, New York, 1962.
22. K. Tai and T. Tagawa, *Ind. Eng. Chem., Prod. R&D,* **22,** 192 (1983).
23. S. K. Gupta, *Numerical Methods for Engineers,* Wiley Eastern, New Delhi, 1994.
24. S. K. Soh and D. C. Sundberg, *J. Polym. Sci., Polym. Chem. Ed.*, **20,** 1299 (1982).
25. S. K. Soh and D. C. Sundberg, *J. Polym. Sci., Polym. Chem. Ed.*, **20,** 1315 (1982).
26. A. B. Ray, D. N. Saraf, and S. K. Gupta, *Polym. Eng. Sci.*, to appear.
27. J. A. Barrie, in *Diffusion in Polymers,* J. Crank and G. S. Park, Eds., Academic Press, London, 1968.
28. S. Onogi, K. Sasaguri, T. Adachi, and S. Ogihara, *J. Polym. Sci.*, **58,** 1 (1962).
29. M. Box, *Computer J.*, **8,** 42 (1965).
30. J. L. Kuester and J. H. Mize, *Optimization Techniques with Fortran,* 1st ed., McGraw-Hill, New York, 1973.

Received October 14, 1993
Accepted January 17, 1994